Biointerface Research in Applied Chemistry
Open-Access Journal (ISSN: 2069-5837)

Article
Volume 14, Issue 6, 2024, 136
https://doi.org/10.33263/BRIAC146.136

Characterization of High-Density Polyethylene (HDPE)-based Biocomposite with Green Seaweed Caulerpa lentillifera as Filler and Polyethylene-grafted-Maleic Anhydride (PE-g-MA) as Coupling Agent

Puji Rizana Ayu Mentari [1], Suharti Suharti [1], Ilham Andreansyah [2], Agus Wedi Pratama [3], Siti Agustina [4], Sona Suhartana [5], Firda Aulya Syamani [5,6,7,*]

[1] Department of Chemistry, State University of Malang, Jl. Semarang No. 5, Malang City, East Java 65145, Indonesia; pujirizanaam@gmail.com (P.R.A.M.); suharti.fmipa@um.ac.id (S.S.);
[2] Faculty of Industrial Technology, Jayabaya University, DKI Jakarta 16452, Indonesia; leonardilham567@gmail.com (I.A.);
[3] Department of Chemistry, Institut Teknologi Sepuluh Nopember, Jl. Kampus ITS, Surabaya, East Java 60117, Indonesia; aguswedi455@gmail.com (A.W.P.);
[4] Research Center for Agroindustry, National Research and Innovation Agency (BRIN), Tangerang Selatan, Banten 15314, Indonesia; siti096@brin.go.id (S.A.);
[5] Research Center for Ecology and Ethnobiology, National Research and Innovation Agency (BRIN), Jl. Raya Jakarta-Bogor Km.46, Cibinong, West Java 16911, Indonesia; sona001@brin.go.id (S.S.);
[6] Research Center for Biomass and Bioproduct, National Research and Innovation Agency (BRIN), Jl. Raya Jakarta-Bogor Km.46, Cibinong, West Java 16911, Indonesia; firda.aulya.syamani@brin.go.id (F.A.S.);
[7] Research Collaboration Center for Marine Biomaterials, Jl. Ir. Sukarno, KM 21, Jatinangor, Sumedang, West Java 45363, Indonesia
* Correspondence: firda.aulya.syamani@brin.go.id (F.A.S.);

Scopus Author ID 56004426100
Received: 22.02.2024; Accepted: 7.07.2024; Published: 10.12.2024

Abstract: Indonesia possesses abundant seaweed resources; however, their use in composites remains limited. This study investigates the impact of incorporating green seaweed (Caulerpa lentillifera) as a filler and polyethylene-grafted-maleic anhydride (PE-g-MA) as a coupling agent on the mechanical, thermal, morphological, water uptake, and soil degradation properties of high-density polyethylene (HDPE) biocomposite. *C. lentillifera* content in the biocomposite was varied from 10% to 40%, PE-g-MA content ranged from 0% to 15%, and *C. lentillifera* particle size was also varied. Results indicate that adding *C. lentillifera* significantly increases the biocomposite's modulus of elasticity (up to 1.63 GPa), thermal stability, and soil degradation resistance (up to 15%). The incorporation of PE-g-MA (up to 5%) effectively reduces water uptake to 0.94%, slightly improves mechanical properties, and enhances interfacial adhesion compared to the un-compatibilized biocomposite. A smaller *C. lentillifera* particle size further decreases water uptake and soil degradation, reaching 0.45% and 1.13%, respectively.

Keywords: seaweed biocomposite; HDPE; PE-g-MA; biocomposites; mechanical and degradation properties.

1. Introduction

Composite materials play a crucial role in various industries due to their enhanced properties, such as superior strength and stiffness compared to their constituent materials [1,2].

Thermoplastic polymer-based composites, particularly those made from high-density polyethylene (HDPE), are widely utilized for their availability, cost-effectiveness, heat resistance, and chemical stability [3]. HDPE, a petroleum-derived plastic polymer, is commonly employed in rigid packaging applications [4]. However, its slow degradation rate raises environmental concerns [5,6].

To address this issue, developing HDPE-based biocomposites incorporating natural fillers has gained attention. These biocomposites offer the potential to enhance biodegradability and reduce reliance on non-renewable resources [7–9]. Biocomposites consist of a continuous matrix phase and a discontinuous reinforcement or filler phase, with at least one component derived from renewable sources [10,11]. Natural fillers, including seaweed, are attractive due to their abundance, low cost, renewability, and processing flexibility [12–15].

Indonesia boasts vast seaweed resources, and one species with promising potential as a filler is Caulerpa. Among the genera of green seaweed, Caulerpa has a large number of species that are found in Indonesia [16,17]. *C. lentillifera*, one of the species of genus Caulerpa, characterized by its grape-like vesicles, thrives in shallow waters and is increasingly utilized in food, medicine, and cosmetics [18–20]. While previous studies have explored the use of other seaweed species in biocomposites [21–23], the application of *C. lentillifera* remains largely unexplored.

A key challenge in developing biocomposites is the inherent incompatibility between hydrophilic fillers and hydrophobic matrices like HDPE, which often leads to high water uptake and compromised mechanical properties. To overcome this, interfacial modification by adding coupling agents, such as polyethylene-grafted-maleic anhydride (PE-g-MA), is crucial [24–26]. PE-g-MA has improved filler-matrix adhesion and reduced water uptake in biocomposites [27,28]. Therefore, this study aims to investigate the effects of incorporating *C. lentillifera* as a filler, varying PE-g-MA content, and adjusting *C. lentillifera* particle size on the mechanical, thermal, water uptake, soil degradation, and morphological properties of HDPE biocomposites.

2. Materials and Methods

2.1. Materials.

Caulerpa lentillifera was collected from Halmahera, North Maluku province, Indonesia. High-density polyethylene (HDPE) HD5218EA (melting point: 130°C, MFI at 190°C/2.16 kg: 18 g/10 min) was obtained from PT. Lotte Chemical Titan Nusantara Indonesia and polyethylene-grafted-maleic anhydride (PE-g-MA) (viscosity: 500 cP at 140°C) were purchased from Merck, Germany.

2.2. Preparation of C. lentillifera powder.

C. lentillifera seaweed was ground into a powder using a Retsch MM 400 Mixer Mill (30 Hz, 15 x 4 minutes) and then sieved. The fine powder used for biocomposite fabrication was the fraction that passed through a 40-mesh sieve but was retained on a 60-mesh sieve. A finer fraction passing through a 60-mesh sieve and retained on an 80-mesh sieve was also used.

2.3. Preparation of biocomposite.

Biocomposites were fabricated using a melt mixing method with a HAAKE Polylab OS Rheomix system. First, HDPE was melted, followed by adding PE-g-MA and *C. lentillifera* powder. The Rheomix was set at 140°C for 10 minutes at 80 rpm. The blended mixture was then processed into dumbbell specimens via a HAAKE MiniJet Pro mini injection molder (cylinder: 160°C, mold: 40°C, 700 bar, 20 seconds) and sheets via a YASUDA hot press (160°C, 20 MPa, 8 minutes). The biocomposite fabrication process is illustrated in Figure 1, while sample codes and compositions with varying *C. lentillifera* content, PE-g-MA content, and particle sizes are detailed in Table 1.

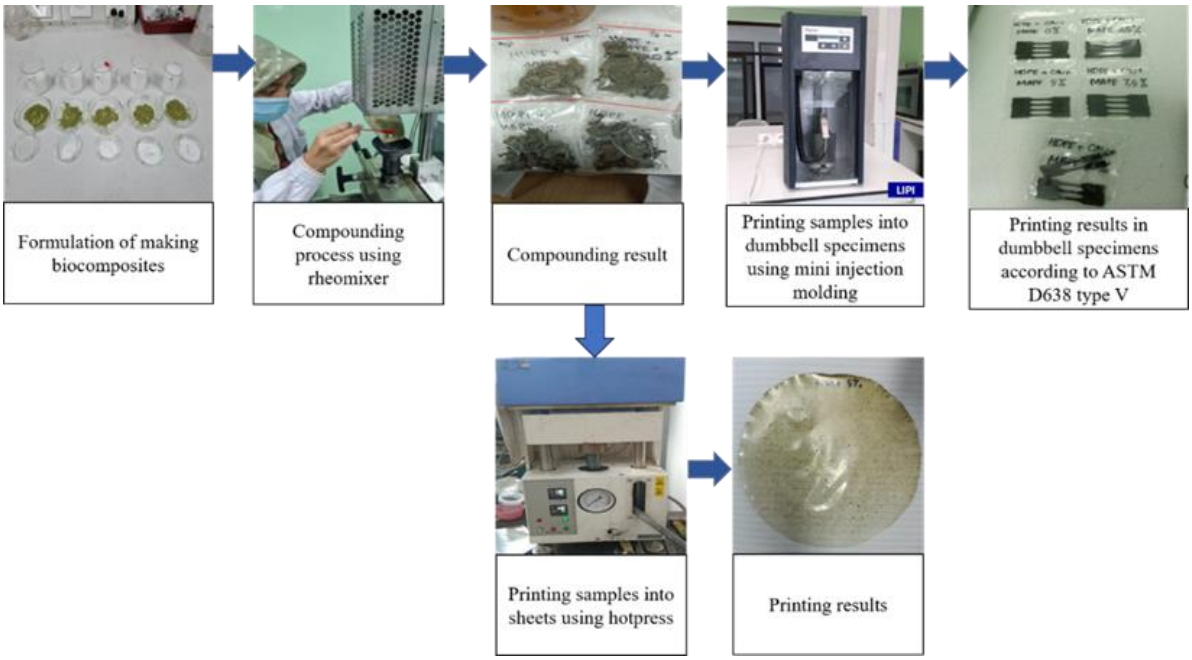

Figure 1. Preparation of making biocomposite.

Table 1. Sample codes and composition of biocomposites.

Sample	Description	Composition (g)		
		HDPE	*C. lentillifera*	PE-g-MA
HDPE	HDPE	50	0	0
HPC 10%	HDPE - PE-g-MA – Caulerpa 10%	44	5	1
HPC 20%	HDPE - PE-g-MA – Caulerpa 20%	39	10	1
HPC 30%	HDPE - PE-g-MA – Caulerpa 30%	34	15	1
HPC 40%	HDPE - PE-g-MA – Caulerpa 40%	29	20	1
HCP 0%	HDPE – Caulerpa - PE-g-MA 0%	45	5	0
HCP 5%	HDPE – Caulerpa - PE-g-MA 5%	44.75	5	0.25
HCP 10%	HDPE – Caulerpa - PE-g-MA 10%	44.5	5	0.5
HCP 15%	HDPE – Caulerpa - PE-g-MA 15%	44.25	5	0.75
HPC large	HDPE - PE-g-MA – Caulerpa[1]	44	5	1
HPC small	HDPE - PE-g-MA – Caulerpa[2]	44	5	1

[1] Caulerpa powder passes a 40 mesh sieve retained by 60 mesh; [2] Caulerpa powder passes a 60 mesh sieve retained by 80 mesh.

2.4. Characterization of biocomposite.

2.4.1. Fourier transform infrared (FTIR).

FTIR analysis was conducted using the attenuated total reflectance (ATR) method to identify the presence of bonds between PE-g-MA and hydroxyl groups in the seaweed. The spectra were collected within the range of 4000 cm^{-1} to 400 cm^{-1}.

2.4.2. Mechanical properties.

Dumbbell-shaped biocomposite specimens, prepared according to ASTM D638 type V, were subjected to tensile testing using a Shimadzu AGS-X Universal Testing Machine (Kyoto, Japan). The tests were performed at a crosshead speed of 5 mm/min with a 5 kN load cell.

2.4.3. Thermal properties.

Thermal stability was evaluated using a Perkin Elmer TGA 4000 thermogravimetric analyzer. Samples were heated from 25°C to 500°C at a rate of 10°C/min. Additionally, thermal transitions were analyzed using a Perkin Elmer DSC 4000 Pyris 1 differential scanning calorimeter. Samples were subjected to a heating-cooling cycle between -20°C and 300°C at a rate of 10°C/min.

2.4.4. Soil burial test.

Samples (2 cm x 2 cm) were buried 5 cm deep in soil (pH 7, relative humidity 84%) for 60 days. Mass measurements and visual observations were conducted every 15 days to assess degradation. The percentage of soil degradability was calculated using Equation 1:

$$\text{Degradability (\%)} = \frac{Wi-Wf}{Wi} \text{ x } 100 \qquad (1)$$

Where Wi is the initial weight (g), and Wf is the final weight (g).

2.4.5. Water uptake.

Water uptake was determined according to ASTM D-570-22. Samples (2 cm x 2 cm) were immersed in water at room temperature for 24 hours. After surface drying, the samples were re-weighed. The percentage of water uptake was calculated using Equation 2:

$$\text{Water uptake (\%)} = \frac{Wf-Wi}{Wi} \text{ x } 100 \qquad (2)$$

Where Wi is the initial weight (g), and Wf is the final weight (g).

2.4.6. Morphology.

The surface morphology of biocomposites with and without PE-g-MA was examined using a Thermo Scientific Quattro S field emission scanning electron microscope (FE-SEM) at 1 kV and 1000x magnification.

3. Results and Discussion

C. lentillifera contains chemical contents, with polysaccharides as a major component [29]. The chemical content of *C. lentillifera* might vary because of their habitat, maturity level, and environmental conditions [30]. The chemical contents of *C. lentillifera* from different sources are presented in Table 2.

Table 2. Chemical contents of *C. lentillifera* from different resources.

Chemical contents of *C. lentillifera*	**Sources**	
	Halmahera, Indonesia [18]	**Okinawa, Japan [31]**
Moisture content	11.94 ± 0.4	-

Chemical contents of *C. lentillifera*	Sources	
	Halmahera, Indonesia [18]	Okinawa, Japan [31]
Ash	31.62 ± 0.4	50
Extractives	11.53 ± 1.44	5.4
α-cellulose	7.95 ± 1.64	5.6
Hemicellulose	35.57 ± 0.37	20.7

3.1. FTIR analysis.

Figure 2 presents the FTIR spectra of HCP 0%, HCP 5%, HCP 15%, and HCP small biocomposites. A summary of the observed peak wavelengths is provided in Table 3. All biocomposites exhibited characteristic biomass peaks at 3356 cm^{-1}, 2917 – 2916 cm^{-1}, 2848 cm^{-1}, 1473 cm^{-1}, and 1462 cm^{-1} [32,33]. The broad absorbance at 3356 cm^{-1} indicates the presence of hydroxyl (O-H) groups from cellulose and hemicellulose in *C. lentillifera* [34–37]. The HDPE matrix contributed to peaks at 2917-2916 cm^{-1} and 2848 cm^{-1}, representing asymmetric and symmetric C-H stretching vibrations, respectively, and peaks at 1473 cm^{-1} and 1462 cm^{-1}, corresponding to C-H bending vibrations [27].

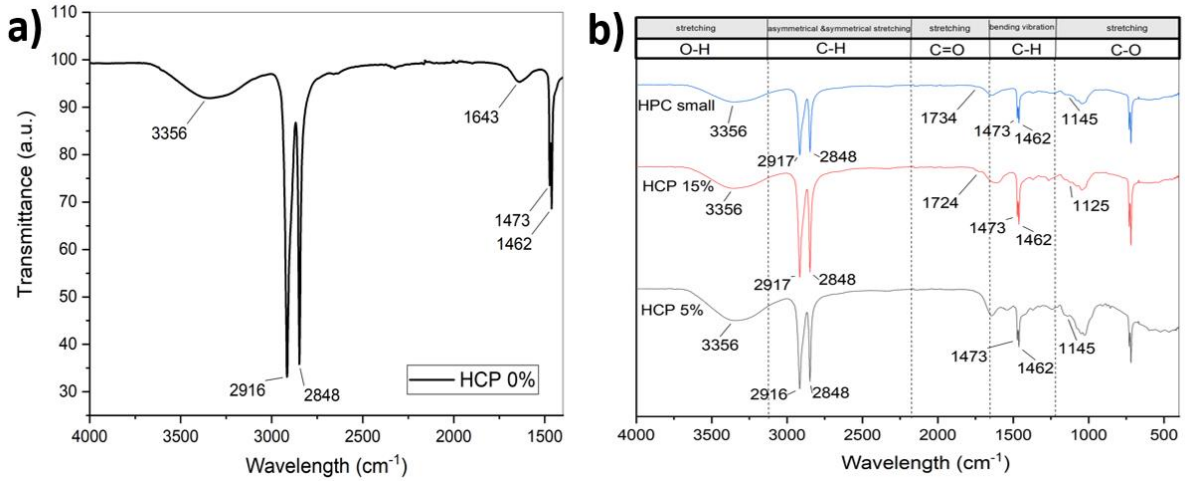

Figure 2. FTIR spectrum of **a)** biocomposites without PE-g-MA; **b)** biocomposites with PE-g-MA.

Table 3. FTIR spectral vibration of HDPE/ *C. lentillifera* biocomposites.

HCP 0% (cm^{-1})	HCP 5% (cm^{-1})	HCP 15% (cm^{-1})	HPC small (cm^{-1})	Possible peak assignments
3356	3356	3356	3356	O-H stretching
2916	2917	2917	2916	asymmetrical stretching vibration C-H
2848	2848	2848	2848	symmetrical stretching vibration C-H
-	-	1724	1734	C=O stretching
1473	1473	1473	1473	bending vibration C-H
1462	1462	1462	1462	bending vibration C-H
-	1145	1125	1145	C-O streching

In biocomposites containing PE-g-MA, distinct peaks emerged around 1724 cm^{-1}–1736 cm^{-1} and 1145 cm^{-1} – 1125 cm^{-1}. These peaks confirm the formation of ester bonds (C=O and C-O stretches) resulting from the esterification reaction between hydroxyl groups in *C. lentillifera* and anhydride groups in PE-g-MA [38–40]. The absence of these peaks in the HCP 0% biocomposite indicates the lack of PE-g-MA in that formulation.

3.2. Mechanical properties.

Figure 3 presents the mechanical properties of HDPE/*C. lentillifera* biocomposites with varying *C. lentillifera* powder content (10%, 20%, 30%, 40%), PE-g-MA content (0%, 5%, 10%, 15%), and *C. lentillifera* particle size. For packaging applications, tensile strength and modulus of elasticity are crucial mechanical characteristics. Adding 40% *C. lentillifera* to HDPE reduced the biocomposite's tensile strength and elongation at break to 18.81 MPa and 2.98%, respectively, while increasing the elastic modulus to 1.63 GPa.

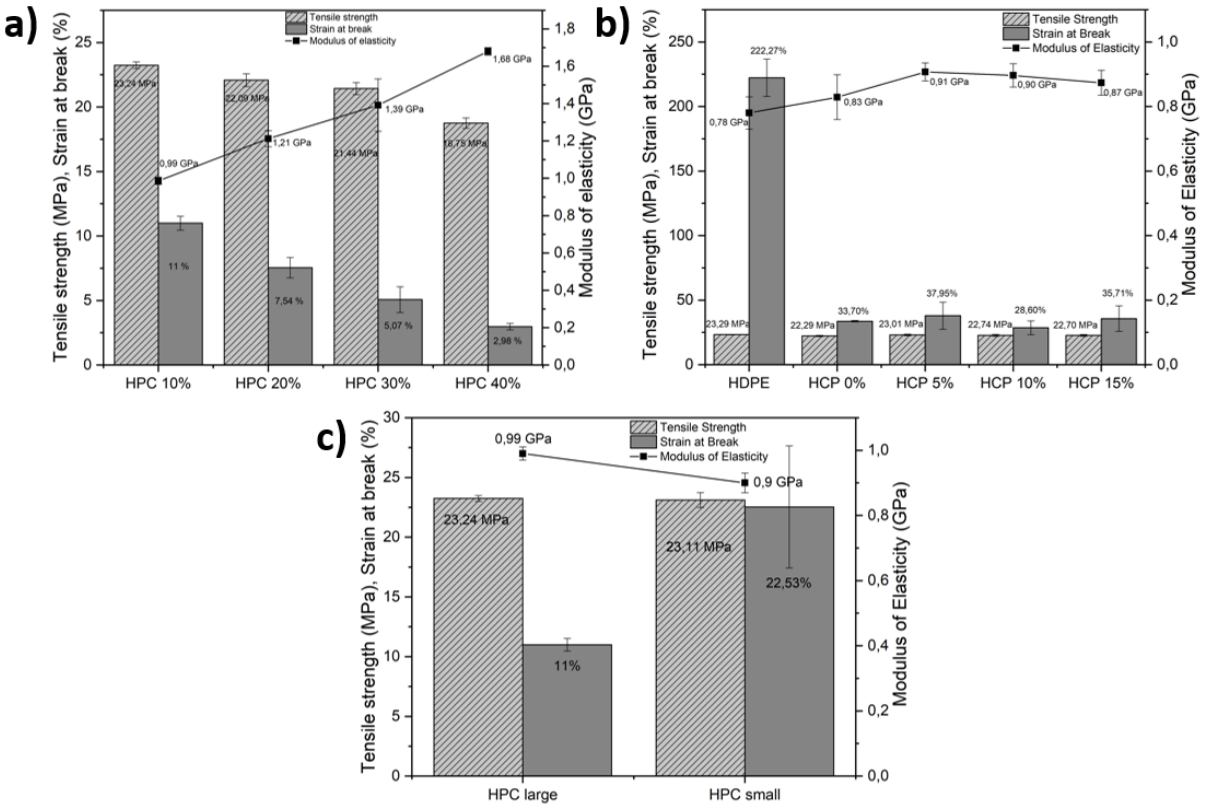

Figure 3. Mechanical properties of HDPE and HDPE biocomposites with a variation of **(a)** *C. lentillifera*; **(b)** PE-g-MA; **(c)** particle size of *C. lentillifera*.

The mechanical properties of biocomposites are influenced by the matrix and filler. Natural fibers, often rich in cellulose, typically act as reinforcing agents. However, *C. lentillifera* contains a higher proportion of hemicellulose (35.57%) than cellulose (7.95%) [18]. Hemicellulose, unlike cellulose, does not significantly contribute to reinforcement. This explains the slight decrease in tensile strength observed in HDPE/*C. lentillifera* biocomposites compared to HDPE-based biocomposites filled with microfibrillated cellulose, which exhibit high flexural strength (43.43-78.97 MPa) and flexural modulus (2.24-3.45 GPa) [41].

The addition of 5% PE-g-MA enhanced the mechanical properties of the biocomposites compared to those without PE-g-MA, consistent with previous findings on HDPE biocomposites [42–44]. This improvement is attributed to increased interfacial bonding between the filler and matrix, facilitated by the formation of bonds between HDPE and the polyethylene segment of PE-g-MA, as well as ester bonds between the maleic anhydride group of PE-g-MA and hydroxyl groups in the seaweed [45]. The grafting reaction mechanism between PE-g-MA and seaweed hydroxyl groups is illustrated in Figure 4. Increasing PE-g-MA content beyond 5% did not yield significant further improvement, suggesting that 5% is an optimal concentration for enhancing mechanical properties.

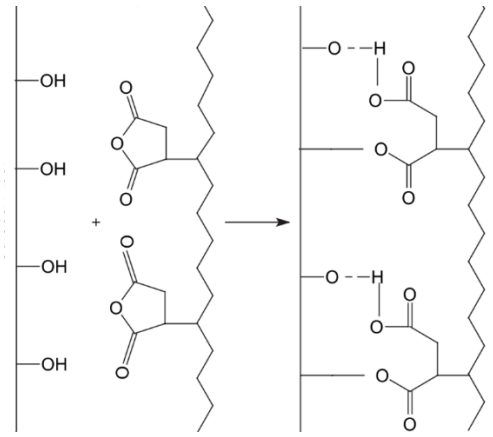

Figure 4. Grafting reaction mechanism between MAPE and the hydroxyl group of seaweed.

The particle size of *C. lentillifera* also affected the biocomposite's mechanical properties. Smaller particles (passing through a 60-mesh sieve but retained on an 80-mesh sieve) resulted in a twofold increase in elongation at break compared to larger particles (passing through a 40-mesh sieve but retained on a 60-mesh sieve). This observation aligns with findings on PVA biocomposites containing Zostera algae fillers [46]. Smaller particle size improves dispersion in the HDPE matrix, enhancing filler-matrix interactions and stress transfer [22].

For flexible packaging applications, which require good tensile strength and elongation at break, the biocomposite with 10% *C. lentillifera*, 5% PE-g-MA, and small particle size is more suitable. For rigid packaging, the biocomposite with 10% *C. lentillifera*, 5% PE-g-MA, and large particle size is preferable due to its higher modulus of elasticity.

3.3. Thermal properties.

3.3.1. DSC analysis.

DSC analysis was employed to evaluate the thermal properties of the HDPE/*C. lentillifera* biocomposites. This technique measures the energy absorbed (endothermic) or released (exothermic) during heating, providing insights into melting and crystallization behavior.

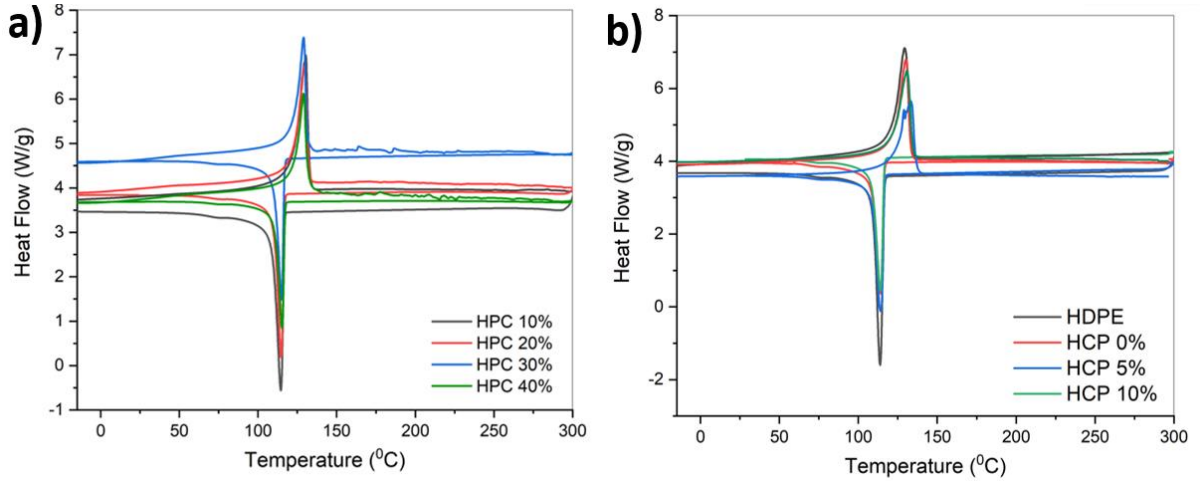

Figure 5. DSC thermogram of HDPE and HDPE biocomposites variation of: **(a)** *C. lentillifera*; **(b)** PE-g-MA.

The impact of *C. lentillifera* and PE-g-MA on the melting temperature (Tm), crystallization temperature (Tc), total melting enthalpy (ΔHm), and total crystallization enthalpy (ΔHc) was investigated. As a semi-crystalline polymer, HDPE's crystal structure can be disrupted by the addition of fillers and coupling agents, potentially altering its thermal

properties [23]. Figure 5 displays the DSC curves for HDPE/*C. lentillifera* biocomposites with varying *C. lentillifera* and PE-g-MA contents, while Table 4 summarizes the corresponding thermal parameters.

Table 4. The value of the thermal parameters of HDPE and HDPE biocomposites is based on the DSC analysis.

Sample	T_m (°C)	ΔH_m (J/g)	T_c (°C)	ΔH_c (J/g)
HPC 10%	130.29	159.25	114.57	-145.09
HPC 20%	129.36	132.52	114.66	-121.01
HPC 30%	129.08	116.38	114.88	-104.65
HPC 40%	128.89	112.53	115.25	-90.48
HDPE	129.31	173.50	113.85	-155.95
HCP 0%	130.13	170.25	114.14	-136.52
HCP 5%	133.05	156.54	114.03	-141.41
HCP 10%	130.92	160.91	113.97	-133.66

The addition of *C. lentillifera* had a negligible effect on the melting and crystallization temperatures compared to pure HDPE (129.31°C and 113.85°C, respectively). However, both *C. lentillifera* and PE-g-MA reduced the ΔHm of the biocomposites, indicating a decrease in crystallinity. Notably, the ΔHm decreased to 112.53 J/g with 40% *C. lentillifera* and 160.91 J/g with 10% PE-g-MA. Conversely, the crystallization enthalpy (ΔHc) increased with the addition of both *C. lentillifera* and PE-g-MA, reaching -90.48 J/g and -133.66 J/g with 40% *C. lentillifera* and 10% PE-g-MA, respectively, suggesting enhanced crystallization behavior compared to pure HDPE.

3.3.2. TGA analysis.

TGA was employed to assess the thermal stability of the biocomposites by monitoring weight loss as a function of temperature. Figure 6 demonstrates that both *C. lentillifera* and PE-g-MA content influenced the thermal degradation behavior. The weight-loss parameters at various temperatures are presented in Tables 5 and 6. The thermal degradation of biocomposites with varying *C. lentillifera* content occurred in three stages, as evidenced by three peaks in the derivative thermogravimetry (DTG) curve. The initial stage, spanning from 25°C to approximately 200°C, involved weight loss primarily due to water evaporation from hydroxyl (-OH) groups in the seaweed [47]. The second stage, occurring between 200°C and 400°C, resulted from the depolymerization of organic components in the seaweed, such as lipids, proteins, carbohydrates, hemicellulose, and cellulose [48]. The final stage, between 400°C and 500°C, involves the thermal degradation of the HDPE matrix [49].

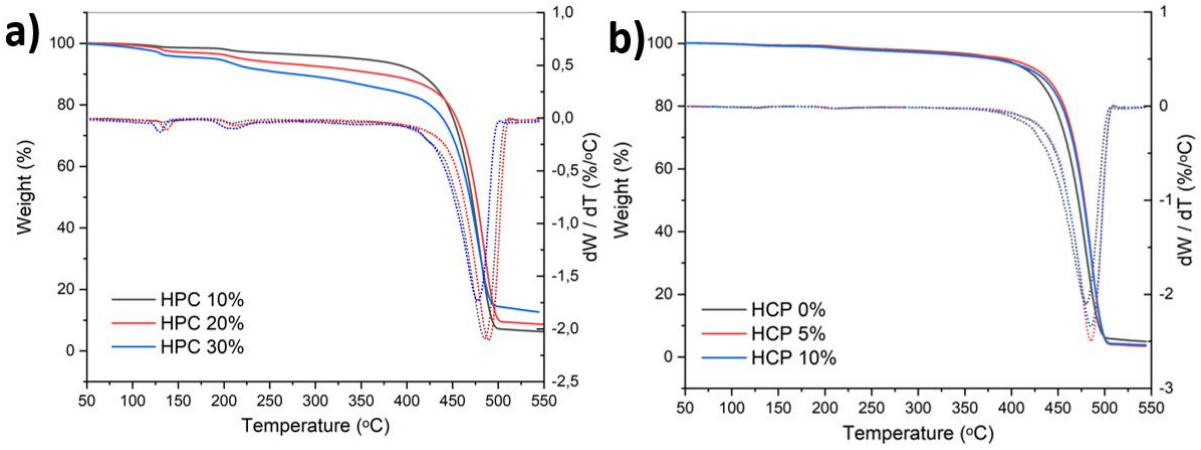

Figure 6. TGA and DTG thermogram of HDPE biocomposites variation: **(a)** *C. lentillifera*; **(b)** PE-g-MA.

Table 5. Value of thermal stability HDPE/*C. lentillifera* biocomposites with a variation of *C. lentillifera* based on the weight loss obtained through TGA and DTG.

Samples	WL stage 1 (%)	WL stage 2 (%)	WL stage 3 (%)	Weight loss (%)	Residue (%)
HPC 10%	1.89	5.95	85.80	93.64	6.36
HPC 20%	3.73	7.92	79.61	91.27	8.73
HPC 30%	5.61	10.96	70.78	87.35	12.65

Table 6. Value of thermal stability HDPE/*C. lentillifera* biocomposites with the variation of PE-g-MA based on the weight loss obtained through TGA and DTG.

Samples	Stage 1 (°C)	WL (%)	Residue (%)
HCP 0%	480.47	95.03	4.97
HCP 5%	485.36	96.56	3.44
HCP 10%	483.67	96.15	3.85

Increasing the *C. lentillifera* content decreased overall weight loss percentage, dropping from 93.64% to 87.35% with 30% seaweed. However, the initial weight loss at the beginning of heating was higher for biocomposites with higher seaweed content due to the increased presence of cellulose and hemicellulose. Conversely, the thermal degradation residue increased with increasing *C. lentillifera* content.

The degradation of HDPE/*C. lentillifera* biocomposites containing PE-g-MA occurred in a single step. Adding 5% PE-g-MA increased the decomposition temperature to 485.36°C, compared to 480.47°C for the biocomposite without PE-g-MA, indicating improved thermal stability. However, the biocomposite with 5% PE-g-MA exhibited a slightly higher weight loss percentage (96.56%) and lower residue (3.44%) than the biocomposite without PE-g-MA (95.03% weight loss, 4.97% residue). This suggests that while PE-g-MA enhances thermal stability, it may also lead to higher degradation at elevated temperatures.

3.4. Soil burial test.

The biocomposite degradation results in soil are presented in Figure 7.

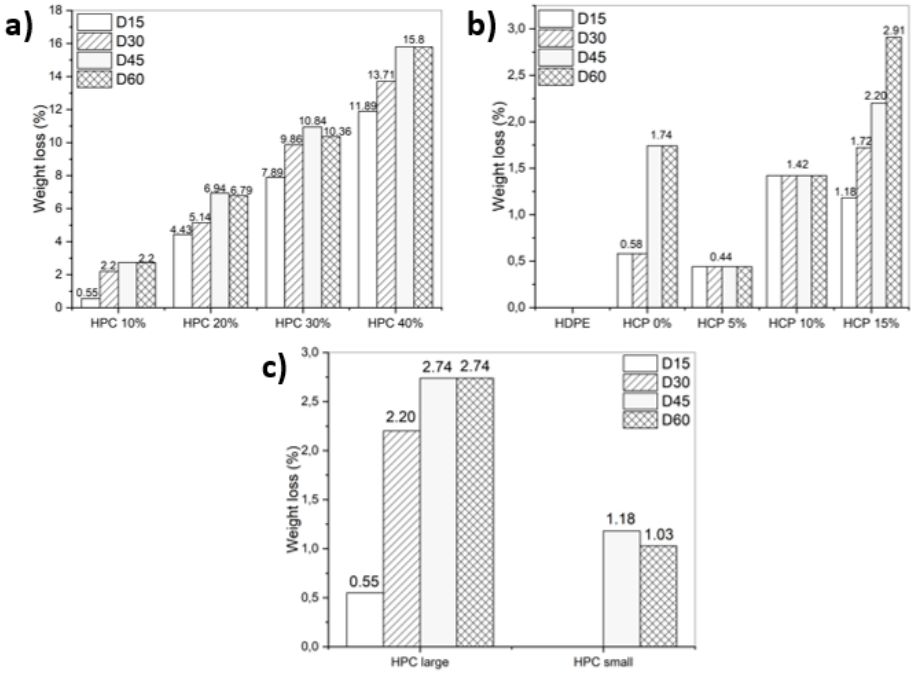

Figure 7. Degradation of HDPE and HDPE/*C. lentillifera* biocomposites on soil with a variation of **(a)** *C. lentillifera*; **(b)** PE-g-MA; **(c)** particle size of *C. lentillifera*.

A higher *C. lentillifera* content resulted in faster degradation, as evidenced by the increased weight loss, reaching up to 15%. This observation aligns with findings on LLDPE biocomposites containing date waste fillers, where increasing natural filler content also led to higher weight loss [50]. The presence of microorganisms in the soil, facilitated by adding EM4 as a microbial consortium, likely contributed to the degradation process. Seaweed with higher cellulose and lignocellulosic content provides more attachment sites for microorganisms, accelerating their growth and the subsequent degradation of the biopolymer. These microorganisms utilize the biopolymer as a carbon source, causing chain scission and fragmentation into lower molecular weight compounds [51].

Figure 7b reveals that biocomposites without PE-g-MA exhibited greater weight loss than those with PE-g-MA. Furthermore, increasing PE-g-MA content led to slightly higher weight loss. However, the 5% PE-g-MA formulation demonstrated the most effective interaction with *C. lentillifera* and HDPE particles, as supported by FTIR analysis (Figure 2b) and the highest elastic modulus values (Figure 3b). This enhanced interaction likely made the biocomposite more resistant to microbial attack, requiring more time for degradation.

Pure HDPE remained undegraded after 60 days due to its hydrophobic long carbon chains, which resist degradation. Adding PE-g-MA up to 15% had minimal impact on the degradability of the biocomposites.

The particle size of *C. lentillifera* powder also influenced degradation. Biocomposites with larger particles exhibited higher degradation (2.74%) compared to those with smaller particles (1.18%). Similar results have been reported for LDPE biocomposites with wood flour and flax straw oil fillers [52]. This can be attributed to the better encapsulation of smaller *C. lentillifera* particles within the polymer matrix, hindering microbial penetration, whereas larger particles may be more loosely connected, facilitating microbial access to the composite.

3.5. Water uptake.

Figure 8 illustrates the water uptake of the biocomposites. Water absorption increased with increasing *C. lentillifera* content, reaching 10.74% at 40% seaweed.

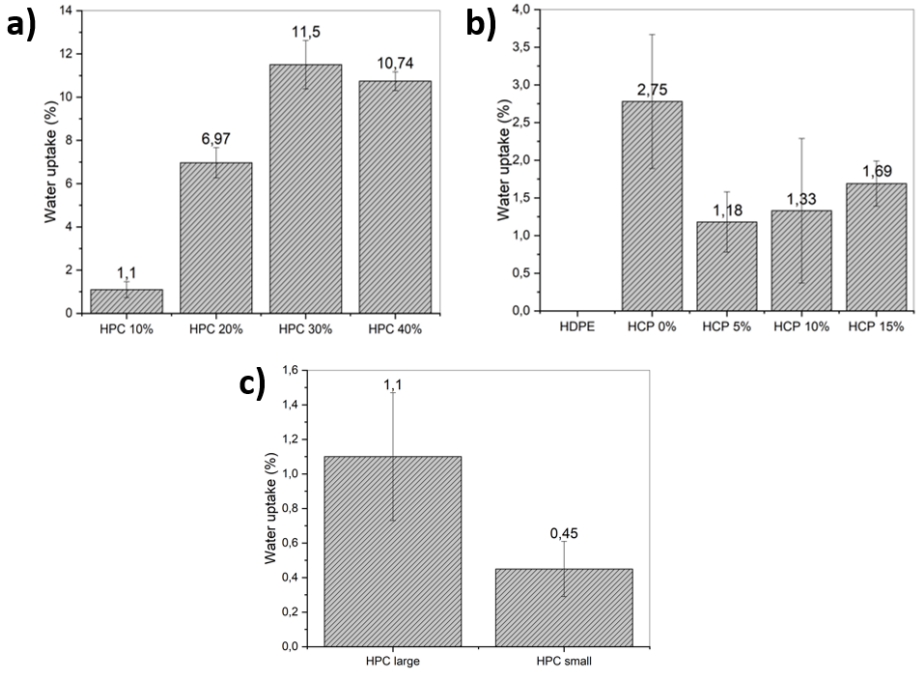

Figure 8. Water uptake of HDPE and HDPE/*C.lentillifera* biocomposites with a variation of **a)** *C. lentillifera*; **b)** PE-g-MA; **c)** particle size of *C. lentillifera*.

This is attributed to the abundance of hydroxyl groups in cellulose and hemicellulose, which are known for their hygroscopic nature [29]. The incorporation of PE-g-MA significantly reduced the water uptake compared to biocomposites without PE-g-MA. This is due to the covalent bonding between the anhydride group in PE-g-MA and the hydroxyl groups in cellulose and hemicellulose, reducing the number of free hydroxyl groups available for water binding [53]. The particle size of *C. lentillifera* also influenced water uptake. Biocomposites with larger particles exhibited a higher water uptake (1.10%) than those with smaller particles. This is likely due to better encapsulation of smaller particles within the polymer matrix, limiting their interaction with water molecules [52].

3.6. Morphology.

The surface morphology of HDPE/*C. lentillifera* biocomposites without PE-g-MA (HCP 0%) and with 5% PE-g-MA (HCP 5%) were examined using field emission scanning electron microscopy (FE-SEM) at 1000x magnification (Figure 9). The biocomposite without PE-g-MA exhibited a rough, uneven surface, with *C. lentillifera* not well-distributed in the HDPE matrix. This observation aligns with previous studies on polyethylene biocomposites [54] and is attributed to poor adhesion between the hydrophobic HDPE matrix and the hydrophilic seaweed filler. Such poor adhesion can lead to the formation of cracks and voids at the interface [42].

In contrast, the biocomposite containing 5% PE-g-MA displayed a more even distribution of *C. lentillifera*, indicating improved interfacial adhesion between the filler and matrix. This improvement is likely due to the PE-g-MA coupling agent facilitating stronger interactions between the two components [55].

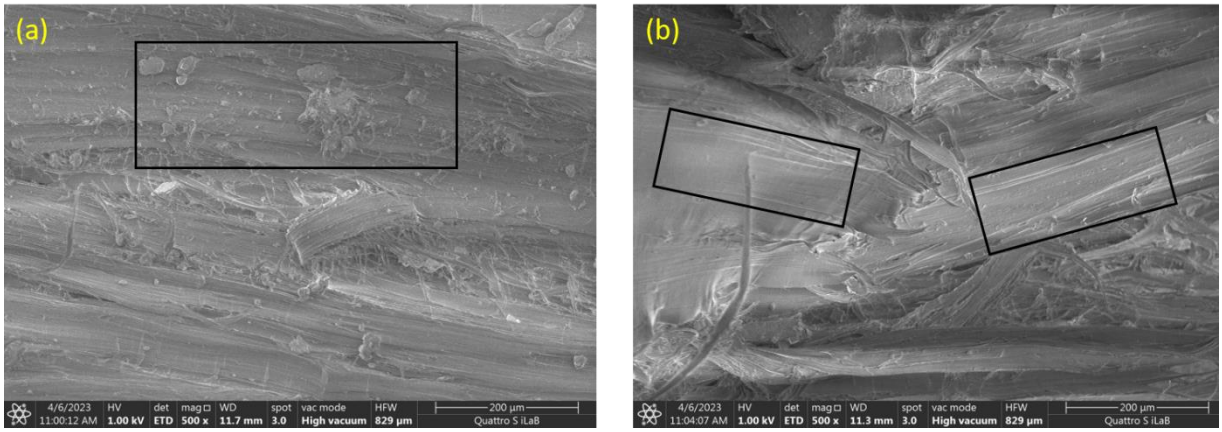

Figure 9. Scanning electronic microscopy (SEM) image of HDPE/C.lentillifera; **(a)** without PE-g-MA (HCP 0%); **(b)** with PE-g-MA 5% (HCP 5%) biocomposite surface at magnifications of 500x

4. Conclusions

Incorporating *C. lentillifera* in HDPE significantly influences the tensile strength, elongation at break, and modulus of elasticity of the resulting biocomposites. The addition of 10% small-particle-size *C. lentillifera* yields a biocomposite with a tensile strength of 23.11 MPa and elongation at a break of 22.53%, making it suitable for flexible packaging applications. Conversely, incorporating 10% large-particle-size *C. lentillifera* results in a biocomposite with a higher modulus of elasticity (0.99 GPa), making it suitable for rigid packaging. Furthermore, adding seaweed enhances the biocomposites' degradation stability,

reducing weight loss to 87.35% and soil degradation to 15.67% over 60 days. The incorporation of PE-g-MA, up to 10%, improves tensile properties and thermal stability due to enhanced interfacial adhesion between HDPE and *C. lentillifera*. Additionally, PE-g-MA effectively reduces the water uptake of the biocomposites. Biocomposites with smaller *C. lentillifera* particle sizes exhibit lower water uptake (0.45%) and soil degradation compared to those with larger particle sizes.

Funding

This project was funded by the Research Organization for Life Sciences and Environment. National Research and Innovation Agency, Indonesia, through the Joint Collaboration Research Program. Number: 39/III.5/HK/2022.

Acknowledgments

The authors also would like to acknowledge the facilities. Scientific and technical support is provided by Advanced Characterization Laboratories Cibinong - Integrated Laboratory of Bioproducts—National Research and Innovation Agency through E-Layanan Sains. Badan Riset dan Inovasi Nasional.

Conflicts of Interest

The authors declare no conflict of interest.

References

1. Thori, P.; Sharma, P.; Bhargava, M. An Approach of Composite Materials in Industrial Machinery: Advantages, Disadvantages and Applications. *Int. J. Res. Eng. Technol.* **2013**, *02*, 350–355, doi:10.15623/ijret.2013.0212060.
2. Xu, X.; Qiu, P.; Sun, M.; Luo, J.; Yu, P.; He, L.; Li, J. Multifunctional Epoxy Resin-Based Composites with Excellent Flexural Strength and X-Ray Imaging Capacity Using Micro/Nano Structured QF-Bi2SiO5 Fillers. *J. Mater. Chem. B* **2023**, *11*, 640–647, doi:10.1039/D2TB02377F.
3. Awan, M.O.; Shakoor, A.; Rehan, M.S.; Gill, Y.Q. Development of HDPE Composites with Improved Mechanical Properties Using Calcium Carbonate and NanoClay. *Phys. B Condens. Matter* **2021**, *606*, 412568, doi:10.1016/j.physb.2020.412568.
4. Spencer, D.B. Household Waste Recycling. *Encycl. Mater. Sci. Technol. (Second Ed.* **2005**, 1–9, doi:10.1016/B978-0-08-047163-1.00582-8.
5. Olam, M. Mechanical and Thermal Properties of HDPE/PET Microplastics, Applications, and Impact on Environment and Life. In *Advances and Challenges in Microplastics*; Salama, E.-S., Ed.; IntechOpen, 2023.
6. Shaari, N.Z.K.; Rahman, N.A.; Taha, A.R.; Alauddin, S.M.; Akhbar, S. Enhancement of Strength and Flexibility of High-Density Polyethylene Using Rubber Leaves. *IOP Conf. Ser. Mater. Sci. Eng.* **2021**, *1053*, 012029, doi:10.1088/1757-899x/1053/1/012029.
7. Mastalygina, E.E.; Pantyukhov, P. V.; Popov, A.A. Biodegradation of Natural Reinforcing Fillers for Polymer Composites. *IOP Conf. Ser. Mater. Sci. Eng.* **2018**, *369*, doi:10.1088/1757-899X/369/1/012044.
8. Laycock, B.; Pratt, S.; Halley, P. A Perspective on Biodegradable Polymer Biocomposites - from Processing to Degradation. *Funct. Compos. Mater.* **2023**, *4*, 10, doi:10.1186/s42252-023-00048-w.
9. Rosli, N.A.; Wan Ishak, W.H.; Ahmad, I. Eco-Friendly High-Density Polyethylene/Amorphous Cellulose Composites: Environmental and Functional Value. *J. Clean. Prod.* **2021**, *290*, 125886, doi:https://doi.org/10.1016/j.jclepro.2021.125886.
10. Zakaria, A.M.; Jamaludin, M.A.; Zakaria, M.N.; Hassan, R.; Bahari, S.A. High Density Polyethylene (HDPE) Composite Mixed with Azadirachta Excelsa (Sentang) Tree Waste Flour: Mechanical and Physical Properties. *IOP Conf. Ser. Earth Environ. Sci.* **2022**, *951*, doi:10.1088/1755-1315/951/1/012045.
11. Zamora-Mendoza, L.; Gushque, F.; Yanez, S.; Jara, N.; Álvarez-Barreto, J.F.; Zamora-Ledezma, C.; Dahoumane, S.A.; Alexis, F. Plant Fibers as Composite Reinforcements for Biomedical Applications. *Bioengineering* 2023, *10*, 804.
12. Halim, N.H.A.; Salim, N. Study on Effect of Different Fiber Loadings on Properties of Seaweed/ Polypropylene Blend Composite. *AIP Conf. Proc.* **2021**, *2339*, doi:10.1063/5.0044195.

13. Khemakhem, M.; Lamnawar, K.; Maazouz, A.; Jaziri, M. Biocomposites Based on Polylactic Acid and Olive Solid Waste Fillers: Effect of Two Compatibilization Approaches on the Physicochemical, Rheological and Mechanical Properties. *Polym. Compos.* **2016**, *39*, 152–163, doi:10.1002/pc.24094.
14. Ismail, S.O.; Akpan, E.; Dhakal, H.N. Review on Natural Plant Fibres and Their Hybrid Composites for Structural Applications: Recent Trends and Future Perspectives. *Compos. Part C Open Access* **2022**, *9*, 100322, doi:https://doi.org/10.1016/j.jcomc.2022.100322.
15. Musa, A.A.; Onwualu, A.P. Potential of Lignocellulosic Fiber Reinforced Polymer Composites for Automobile Parts Production: Current Knowledge, Research Needs, and Future Direction. *Heliyon* **2024**, *10*, e24683, doi:https://doi.org/10.1016/j.heliyon.2024.e24683.
16. Darmawan, M.; Zamani, N.P.; Irianto, H.E.; Madduppa, H. DIVERSITY AND ABUNDANCE OF GREEN SEAWEED Caulerpa (Chlorophyta) ACROSS INDONESIAN COASTAL WATERS WITH DIFFERENT NUTRIENT LEVELS: Bintan Island, Jepara, and Osi Island. *J. Ilmu dan Teknol. Kelaut. Trop.* **2022**, *14*, 273–290.
17. Tapotubun, A.M.; Matrutty, T.E.A.A.; Riry, J.; Tapotubun, E.J.; Fransina, E.G.; Mailoa, M.N.; Riry, W.A.; Setha, B.; Rieuwpassa, F. Seaweed Caulerpa Sp Position as Functional Food. *IOP Conf. Ser. Earth Environ. Sci.* **2020**, *517*, 1–8, doi:10.1088/1755-1315/517/1/012021.
18. Mentari, P.R.A.; Andreansyah, I.; Amanda, P.; Marlina, R.; Agustina, S.; Syamani, F.A.; Suharti, S. Cellulose Isolation and Characterization of Green Seaweed *C. lentillifera* From. *J. Bahan Alam Terbarukan* **2023**, *12*, 112–119, doi:https://doi.org/10.15294/jbat.v12i2.44578.
19. Jumsurizal; Ilhamdy, A.F.; Anggi; Astika Karakteristik Kimia Rumput Laut Hijau (Caulerpa Racemosa & Caulerpa Taxifolia) Dari Laut Natuna, Kepulauan Riau, Indonesia. *J. Akuatika Indones.* **2021**, *6*, 19–24, doi:https://doi.org/10.24198/jaki.v6i1.30008.
20. Baghel, R.S.; Choudhary, B.; Pandey, S.; Pathak, P.K.; Patel, M.K.; Mishra, A. Rehashing Our Insight of Seaweeds as a Potential Source of Foods, Nutraceuticals, and Pharmaceuticals. *Foods* 2023, *12*, 3642.
21. Luan, L.; Wu, W.; Wagner, M.H.; Mueller, M. Seaweed as Novel Biofiller in Polypropylene Composites. *J. Appl. Polym. Sci.* **2010**, *118*, 997–1005, doi:10.1002/app.32462.
22. Hassan, M.M.; Mueller, M.; Wagners, M.H. Exploratory Study on Seaweed as Novel Filler in Polypropylene Composite. *J. Appl. Polym. Sci.* **2008**, *109*, 1242–1247, doi:10.1002/app.28287.
23. Burhani, D.; Sudarmanto; Wijayanto, A.; Andreansyah, I.; Widyawati, Y.; Nurhamiyah, Y.; Fransiska, D.; Agustina, S.; Banar Kusumaningrum, W.; Fatriasari, W.; et al. Utilization of Indonesian Seaweed in Polyethylene-Based Composite with Coconut Husk Powder as Bio-Compatibilizer. *Mater. Today Proc.* **2023**, doi:https://doi.org/10.1016/j.matpr.2023.03.765.
24. Ilyas, R.A.; Sapuan, S.M.; Harussani, M.M.; Hakimi, M.Y.A.Y.; Haziq, M.Z.M.; Atikah, M.S.N. Polylactic Acid (PLA) Biocomposite : Processing , Additive. *Polymers (Basel).* **2021**, *13*, 1326, doi:10.3390/polym13081326.
25. Chairi, M.; Bahaoui, J. El; Hanafi, I.; Cabrera, F.M.; Bella, G. Di Composite Materials: A Review of Polymer and Metal Matrix Composites, Their Mechanical Characterization, and Mechanical Properties. In *Next Generation Fiber-Reinforced Composites - New Insights*; Li, L., Pereira, A.B., Pereira, A.L., Eds.; IntechOpen: Rijeka, 2023; p. Ch. 2 ISBN 978-1-80356-921-5.
26. Sianturi, K.Y.; Nugraha, A.F.; Sianturi, K.Y.; Nugraha, A.F.; Kristaura, B.; Chalid, M. Enhancing Compatibility and Mechanical Properties of Natural Rubber Composites. *J. Mater. Explor. Find.* **2023**, *2*, 17–23, doi:10.7454/jmef.v2i1.1029.
27. Hassan, N.R.N.; Ismail, N.M.; Nuruzzaman, D.M.; Razali, N.M.; Ghazali, S. The Effect of MAPE Compatibilizer Agent on the Tensile Strength of Recycled PET/HDPE Plastic Composite. In Proceedings of the iMEC-APCOMS 2019; Osman Zahid, M.N., Abd. Aziz, R., Yusoff, A.R., Mat Yahya, N., Abdul Aziz, F., Yazid Abu, M., Eds.; Springer Singapore: Singapore, 2020; pp. 484–489.
28. Pearson, A.; Duncan, M.; Hammami, A.; Naguib, H.E. Interfacial Adhesion and Thermal Stability of High-Density Polyethylene Glass Fiber Composites. *Compos. Sci. Technol.* **2022**, *227*, 109570, doi:https://doi.org/10.1016/j.compscitech.2022.109570.
29. Honwichit, O.; Ruengsaengrob, P.; Buathongjan, C.; Charoensiddhi, S. Influence of Extraction Methods on the Chemical Composition and Antioxidant Activity of Polysaccharide Extracts from Discarded Sea Grape (Caulerpa Lentillifera). *J. Fish. Environ.* **2022**, *46*, 169–179.
30. Ito, K.; Hori, K. Seaweed: Chemical Composmon and Potential Food Uses. *Food Rev. Int.* **1989**, *5*, 101–144, doi:10.1080/87559128909540845.
31. Rabemanolontsoa, H.; Saka, S. Comparative Study on Chemical Composition of Various Biomass Species. *RSC Adv.* **2013**, *3*, 3946–3956, doi:10.1039/c3ra22958k.
32. Pratama, A.W.; Mulyono, T.; Piluharto, B.; Widiastuti, N.; Mahardika, M.; Ali, B.T.I.; Asranudin; Allouss, D.; El Alaoui-Elbalrhiti, I. Potential of Cellulose from Wood Waste for Immobilization Saccharomyces Cerevisiae in Bioethanol Production. *J. Indian Chem. Soc.* **2023**, *100*, 101106, doi:10.1016/J.JICS.2023.101106.
33. Pratama, A.W.; Mahardika, M.; Widiastuti, N.; Piluharto, B.; Ilyas, R.A.; Sapuan, S.M.; Amelia, D.; Firmanda, A. Isolation and Characterization of Highly Thermal Stable Microcrystalline Cellulose Derived from Belulang Grass (Eleusine Indica). *Case Stud. Chem. Environ. Eng.* **2024**, *9*, 100743,

doi:10.1016/J.CSCEE.2024.100743.
34. Arnata, I.W.; Suprihatin, S.; Fahma, F.; Richana, N.; Sunarti, T.C. Cationic Modification of Nanocrystalline Cellulose from Sago Fronds. *Cellulose* **2020**, *27*, 3121–3141.
35. Pratama, A.W.; Piluharto, B.; Mahardika, M.; Widiastuti, N.; Firmanda, A.; Norrrahim, M.N.F. Comparative Study of Oxidized Cellulose Nanofibrils Properties from Diverse Sources via TEMPO-Mediated Oxidation. *Case Stud. Chem. Environ. Eng.* **2024**, *10*, 100823, doi:10.1016/J.CSCEE.2024.100823.
36. Pratama, A.W.; Piluharto, B.; Indarti, D.; Haryati, T.; Addy, H.S. Pengaruh Konsentrasi Asam Terhadap Sifat Fisik Dan Muatan Permukaan Selulosa Termodifikasi. *ALCHEMY J. Penelit. Kim.* **2019**, *15*, 315–328, doi:10.20961/ALCHEMY.15.2.33756.315-328.
37. Pratama, A.W.; Addy, H.S.; Widiastuti, N.; Widyanto, A.R.; Ratnasari, A.; Indarti, D.; Piluharto, B. Cellulose Nanofibrils from Corncobs and Their Nanocomposite with Alginate : Study of Swelling Behavior. *Biointerface Res. Appl. Chem.* **2024**, *14*, 4–21, doi:10.33263/BRIAC141.004.
38. Singh, A.A.; Palsule, S. Coconut Fiber Reinforced Chemically Functionalized High-Density Polyethylene (CNF/CF-HDPE) Composites by Palsule Process. *J. Compos. Mater.* **2014**, *48*, 3673–3684, doi:10.1177/0021998313513045.
39. Firmanda, A.; Mahardika, M.; Fahma, F.; Amelia, D.; Pratama, A.W.; Amalia, N.; Syafri, E.; Achaby, M. El Cellulose-Enriched Ascorbic Acid for Wound Dressing Application: Future Medical Textile. *J. Appl. Polym. Sci.* **2024**, *141*, e56013, doi:10.1002/APP.56013.
40. Holilah; Asranudin; El Messaoudi, N.; Ulfa, M.; Hamzah, A.; Hamid, Z.A.A.; Ramadhani, D.V.; Suryanegara, L.; Mahardika, M.; Melenia, A.T.; et al. Fabrication a Sustainable Adsorbent Nanocellulose-Mesoporous Hectorite Bead for Methylene Blue Adsorption. *Case Stud. Chem. Environ. Eng.* **2024**, *10*, 100850, doi:10.1016/J.CSCEE.2024.100850.
41. Zhang, B.; Bu, X.; Wang, R.; Shi, J.; Chen, C. High Mechanical Properties of Micro Fibrillated Cellulose / HDPE Composites Prepared with Two Different Methods. *Cellulose* **2021**, *28*, 5449–5462, doi:10.1007/s10570-021-03885-9.
42. Husseinsyah, S.; Azmin, A.; Ismail, H. Effect of Maleic Anhydride-Grafted-Polyethylene (MAPE) and Silane on Properties of Recycled Polyethylene/Chitosan Biocomposites. *Polym. Plast. Technol. Eng.* **2013**, *52*, 168–174, doi:10.1080/03602559.2012.734362.
43. Zhao, X.; Li, R.K.Y.; Bai, S.L. Mechanical Properties of Sisal Fiber Reinforced High Density Polyethylene Composites: Effect of Fiber Content, Interfacial Compatibilization, and Manufacturing Process. *Compos. Part A Appl. Sci. Manuf.* **2014**, *65*, 169–174, doi:10.1016/j.compositesa.2014.06.017.
44. Zabihzadeh, M.; Dastoorian, F.; Ebrahimi, G. Effect of MAPE on Mechanical and Morphological Properties of Wheat Straw/HDPE Injection Molded Composites. *J. Reinf. Plast. Compos.* **2010**, *29*, 123–131, doi:10.1177/0731684408096426.
45. Obasi, H.C. Tensile and Biodegradable Properties of Extruded Sorghum Flour Filled High Density Polyethylene Films. *Acad. Res. Int.* **2013**, *4*, 78.
46. Chiellini, E.; Cinelli, P.; Ilieva, V.I.; Zimbardi, F.; Kanellopoulos, N.; Wilde, B. De; Verstichel, S.; Pipino, A.; Anders, B.; Sassi, J.F. Hybrid Composites Based on Fibres of Marine Origin. *Int. J. Mater. Prod. Technol.* **2009**, *36*, 47, doi:10.1504/ijmpt.2009.027819.
47. Carpio, R.B.; Zhang, Y.; Kuo, C.T.; Chen, W.T.; Schideman, L.C.; de Leon, R.L. Characterization and Thermal Decomposition of Demineralized Wastewater Algae Biomass. *Algal Res.* **2019**, *38*, 101399, doi:10.1016/j.algal.2018.101399.
48. Khan, N.; Sudhakar, K.; Mamat, R. Thermogravimetric Analysis of Marine Macroalgae Waste Biomass as Bio-Renewable Fuel. *J. Chem.* **2022**, *2022*, 1–9, doi:10.1155/2022/6417326.
49. Koffi, A.; Mijiyawa, F.; Koffi, D.; Erchiqui, F.; Toubal, L. Mechanical Properties, Wettability and Thermal Degradation of HDPE/Birch Fiber Composite. *Polymers (Basel).* **2021**, *13*, doi:10.3390/polym13091459.
50. Alshabanat, M. Morphological, Thermal, and Biodegradation Properties of LLDPE/Treated Date Palm Waste Composite Buried in a Soil Environment. *J. Saudi Chem. Soc.* **2019**, *23*, 355–364, doi:10.1016/j.jscs.2018.08.008.
51. Arutchelvi, J.; Sudhakar, M.; Arkatkar, A.; Doble, M.; Bhaduri, S.; Uppara, P.V. Biodegradation of Polyethylene and Polypropylene. *Indian J. Biotechnol.* **2008**, *7*, 9–22.
52. Zykova, A.K.; Pantyukhov, P. V.; Kolesnikova, N.N.; Monakhova, T. V.; Popov, A.A. Influence of Filler Particle Size on Physical Properties and Biodegradation of Biocomposites Based on Low-Density Polyethylene and Lignocellulosic Fillers. *J. Polym. Environ.* **2018**, *26*, 1343–1354, doi:10.1007/s10924-017-1039-9.
53. Zabihzadeh, S.M. Water Uptake and Flexural Properties of Natural Filler/HDPE Composites. *BioResources* **2010**, *5*, 316–323.
54. Tanjung, D.; Jamarun, N.; Arief, S.; Hermansyah, A.; Ritonga, A.H.; Isfa, B. Influence of LLDPE-g-MA on Mechanical Properties, Degradation Performance and Water Absorption of Thermoplastic Sago Starch Blends. *Indones. J. Chem.* **2022**, *22*, 171–178, doi:10.22146/ijc.68558.
55. Ismail, A.B.; Bakar, H.B.A.; Shafei, S.B. Comparison of LDPE/Corn Stalk with Eco Degradant and LDPE/Corn Stalk with MAPE: Influence of Coupling Agent and Compatibiliser on Mechanical Properties. *Mater. Today Proc.* **2020**, *31*, 360–365, doi:10.1016/j.matpr.2020.06.234.